Journal of Neurochemistry, 2005, **94**, 896–905 doi:10.1111/j.1471-4159.2005.03224.x

Dicer and eIF2c are enriched at postsynaptic densities in adult mouse brain and are modified by neuronal activity in a calpain-dependent manner

Giovanni Lugli,* John Larson,* Maryann E. Martone,† Ying Jones† and Neil R. Smalheiser*

**University of Illinois at Chicago, UIC Psychiatric Institute, Chicago, Illinois, USA*

†*Department of Neurosciences, National Center for Microscopy and Imaging Research, University of California, San Diego, California, USA*

Abstract

We have hypothesized that small RNAs may participate in learning and memory mechanisms. Because dendritic spines are important in synaptic plasticity and learning, we asked whether dicer, the rate-limiting enzyme in the formation of small RNAs, is enriched within dendritic spines. In adult mouse brain, dicer and the RNA-induced silencing complex (RISC) component eIF2c were expressed in the somatodendritic compartment of principal neurons and some interneurons in many regions, and dicer was enriched in dendritic spines and postsynaptic densities (PSDs). A portion of dicer and eIF2c were associated with each other and with fragile X mental retardation protein (FMRP), as assessed by co-immunoprecipitation. Calpain I treatment of recombinant dicer or immunopurified brain dicer caused a marked increase in RNAse III activity. Purified PSDs did not exhibit RNAse III activity, but calpain caused release of dicer from PSDs in an enzymatically active form, together with eIF2c. NMDA stimulation of hippocampal slices, or calcium treatment of synaptoneurosomes, caused a 75 kDa dicer fragment to appear in a calpain-dependent manner. The findings support a model whereby acute neuronal stimulation at excitatory synapses increases intracellular calcium, which activates calpain, which liberates dicer and eIF2c bound to PSDs. This supports the hypothesis that dicer could be involved in synaptic plasticity.

Keywords: learning, microRNA, plasticity, RNA-induced silencing complex, RNA interference, synapse.

J. Neurochem. (2005) **94,** 896–905.

RNA interference (RNAi) is a sequence-specific, long-lasting, post-transcriptional mechanism of gene regulation (Dykxhoorn *et al*. 2003) that can be elicited by double-stranded RNA (e.g. sense–antisense RNA pairs) or by the microRNA family of short trans-acting antisense RNA transcripts (Lai 2003; Bartel 2004). Sense-antisense pairs are processed by dicer (Bernstein *et al*. 2001) into small interfering RNAs (siRNAs). MicroRNA genes are transcribed as precursors that are processed by a nuclear RNAse III enzyme (Drosha) to form ~70 nt hairpins, which are exported to the cytoplasm and further processed by dicer into mature 17–24 nt microRNAs. siRNAs and microRNAs silence target mRNAs via incorporation into the RNA-induced silencing complex (RISC), eliciting mRNA cleavage or arresting mRNA translation.

Since we proposed that RNAi may have a physiological role in regulating brain functions, particularly learning and memory, in the adult mammalian CNS (Smalheiser *et al*. 2001), accumulating evidence strongly supports a role for small RNAs in adult brain.

(i) About 200 mammalian microRNAs have been discovered so far, and many are expressed in adult brain (Lagos-Quintana *et al*. 2002; Dostie *et al*. 2003; Krichevsky *et al*. 2003; Kim *et al*. 2004; Miska *et al*. 2004; Sempere *et al*. 2004).

Received February 2, 2005; revised manuscript received March 25, 2005; accepted March 30, 2005.

Address correspondence and reprint requests to Neil R. Smalheiser, University of Illinois at Chicago, UIC Psychiatric Institute, MC 912, 1601 W. Taylor Street, Room 285, Chicago, Illinois, USA.
E-mail: smalheiser@psych.uic.edu

Abbreviations used: FMRP, fragile X mental retardation protein; LTP, long-term potentiation; PSD, postsynaptic density; RISC, RNA-induced silencing complex; RNAi, RNA interference; dsRNA, double-stranded RNA; siRNA, small interfering RNA.

(ii) RNAi can be experimentally elicited in postmitotic mammalian neurons and can down-regulate genes both *in vitro* and *in vivo* (e.g. Krichevsky and Kosik 2002; Makimura *et al*. 2002; Hommel *et al*. 2003). RNAi elicited in postmitotic neurons persists for at least three weeks (Omi *et al*. 2004).

(iii) Fragile X mental retardation protein (FMRP) associates with dicer, microRNAs and RISC components including Ago 1 and 2 in *Drosophila* and the Ago homolog eIF2c in mammals (Caudy *et al*. 2002, 2003; Ishizuka *et al*. 2002). FMRP associates with brain polysomes and regulates protein synthesis at dendritic spines (Greenough *et al*. 2001), and microRNAs have also been found to be associated with mouse brain polysomes (Kim *et al*. 2004; Nelson *et al*. 2004). Regulation of protein synthesis at dendritic spines is critically important for learning and memory (Martone *et al*. 1996; Greenough *et al*. 2001; Steward and Schuman 2003).

These findings suggest the possibility that small RNAs might regulate mRNA stability and/or translation at dendritic spines. In the present study, we demonstrate in adult mouse brain that dicer is localized in dendritic spines, particularly at postsynaptic densities, and that its localization and activity are modulated by the calcium-dependent protease, calpain, in response to neuronal stimulation. This supports the notion that the RNAi pathway may participate in long-term plasticity mechanisms triggered by transient calcium signals at synapses.

Materials and methods

Subcellular fractionation

Brains from male mice (2 months old) were Dounce homogenized (35 strokes) in HB buffer (50 mM HEPES, pH 7.5, 125 mM NaCl, 100 mM sucrose, 2 mM K Acetate, 10 mM EDTA, 2 mM phenylmethylsulfonyl fluoride, 10 mM *N*-ethylmaleimide, 10 μg/mL leupeptin, 1 μg/mL pepstatin A, 2 μg/mL aprotinin). Crude homogenate was centrifuged (20 000 *g*, 30 min, 4°C) and the supernatant decanted ('cytosol' fraction). In some cases, cytosol was enriched for dicer by ammonium sulfate precipitation (30%) followed by desalting on a G-50 column. Protein was determined by Lowry assay. Samples were precipitated with a sevenfold excess of methanol overnight at −20°C and dissolved in sodium dodecyl sulfate–polyacrylamide gel electrophoresis buffer with 1% dithiothreitol for loading on sodium dodecyl sulfate–polyacrylamide gel electrophoresis gels. Synaptosomes were isolated by sucrose gradient fractionation (Smalheiser and Collins 2000). Synaptosomes were subjected to hypotonic lysis (kept overnight at −80C in 6 mM Tris-HCl, pH 8.0), pelleted (20 000 *g*, 30 min, 4°C), resuspended in HB containing 1% Triton X-100 for 45 min on ice with shaking; and finally pelleted and rinsed twice with HB (lacking protease inhibitors) to obtain purified postsynaptic densities. Equal amounts of protein in each fraction were precipitated with methanol, dissolved in sodium dodecyl sulfate–polyacrylamide gel electrophoresis buffer under reducing conditions, separated on 4–20% gradient polyacrylamide gels (Criterion, Bio-Rad, Hercules, CA, USA), and transferred to polyvinylidene difluoride membranes (Amersham, Piscataway, NJ, USA) for western blotting analyses. Synaptoneurosome preparation was modified from Weiler *et al*. (1997). Forebrains were Dounce homogenized (5–7 strokes) in a 10-fold excess of HB and passed successively through four different nylon filters (149, 60, 30, 10 μm). Filtrate was centrifuged (4000 *g*, 1 min, 4°C) then the supernatant was spun (20 000 *g*, 4 min, 4°C) to obtain synaptoneurosomes.

Antibodies

A peptide was synthesized corresponding to the C-terminal eight amino acids of dicer (identical in mouse and human), conjugated to KLH and used to raise polyclonal antibodies in rabbits (Covance, Denver, PA, USA). Similarly, a peptide corresponding to the C-terminal 16 amino acids of eIF2c1 was used as antigen in rabbits (the C-terminal 16 amino acids are identical in eIF2c2; there is one mismatch in eIF2c3 and four mismatches in eIF2c4). The antibodies were affinity-purified on peptide affinity columns before use. For immunoprecipitation, brain cytosol (200 μL, 2.5 mg/mL) was incubated with anti-dicer antibody (5 μL, 0.025 mg/mL) or anti-eIF2c antibody overnight at 4°C with rocking. Protein A agarose beads were added (10 μL), incubated 2 h and rinsed twice with HB buffer. Alternatively, primary antibodies were covalently attached to agarose beads using a hydrazide coupling kit (Bio-Rad). As negative controls, assays were conducted in the absence of primary or secondary antibodies, in the absence of brain extract, or using an irrelevant primary antibody (anti-reelin antibody G10).

For western blotting, blots were blocked in 1% non-fat dry milk for 1 h, room temperature, incubated with primary antibody [anti-dicer antibody (1:500), anti-eIF2c (1:50 000), mouse anti-FMRP antibody (1:3000, Clontech, Mountain View, CA, USA) or anti-PSD-95 monoclonal antibody (1: 60 000, Clontech)] overnight with rocking at 4°C and rinsed. Goat anti-rabbit IgG (peroxidase conjugated; Sigma A0545, sigma, St Louis, MO, USA) or goat anti-mouse IgG (peroxidase conjugated; Chemicon, Temecula, CA, USA) was added at 1:40 000–50 000 for 2 h and rinsed. Finally, blots were incubated in ECL-Plus reagent (Amersham) and exposed to film (Hyperfilm ECL, Amersham). As a negative control, primary antibody was omitted and/or irrelevant antibodies were used instead.

RNAse III assay

Uniformly radiolabeled dsRNA substrate was prepared per manufacturer's instructions (dicer siRNA generation kit, GTS, San Diego, CA, USA or MEGAscript RNAi Kit, Ambion, Austin, TX, USA). Briefly, dsRNA substrate (500 or 700 bp) was prepared using 0.75 mM UTP and 4 μM [^{32}P]UTP (800 Ci/mmole, Amersham). Substrate was purified in low melting point agarose gels, cutting out the band, and RNA was recovered with chloroform/phenol extraction and ethanol precipitation. RNase III assay was performed in 30 μL at 37°C using [^{32}P]dsRNA in 50 mM NaCl, 10 mM tris-HCl pH 7.0, 0.1 mM EDTA, 1 mM ATP, 3% SUPERase-In (Ambion), 2.5–5 mM $MgCl_2$, 2.5 mM $CaCl_2$. In some cases, calpain I (3 U/mL, from human plasma, Sigma) and/or calpeptin (dissolved in dimethylsulfoxide, used at 100 μg/mL, Calbiochem) were added. Recombinant human dicer (3 U, GTS) was used as a positive control. Aliquots were taken at the indicated times and the reaction stopped with equal amount of non-denaturing gel loading buffer

(62.5 mM Tris-HCl pH 8.0, 25% glycerol, 5 mM EDTA, 0.2% Bromophenol blue, 0.2% Xylene Cyanol FF). Samples were analyzed on 4–20% polyacrylamide-TBE gels (Criterion TBE, Bio-Rad) or 3.5% agarose-TBE gels. Polyacrylamide gels were autoradiographed, visualized on a STORM 840 Optical Scanner (Amersham) and quantified using IMAGEQUANT software (Molecular Dynamics, Sunnyvale CA, USA). Alternatively, agarose gels were stained with ethidium bromide (polyacrylamide gels were stained with Syber Gold, Molecular Probes, Inc., Eugene, OR, USA) and bands of interest were excised and counted on a scintillation counter (Tri-Carb-2100TR, Packard, Meriden, CT, USA).

Light microscopic immunocytochemistry

C57BL/6 mice (Jackson Laboratories, Bar Harbour, Maine, USA), 1 month old, were perfused transcardially with oxygenated Ringers followed by 4% paraformaldehyde in 0.1 M phosphate buffer containing 0.15 M saline, pH 7.2 and postfixed 1–2 h on ice. Sagittal vibratome sections were cut (80 μm), washed 3 × 10 min in phosphate-buffered saline, then blocked in phosphate-buffered saline containing 3% normal donkey serum, 1% bovine serum albumin and 0.2% Triton X-100 for 30 min on ice. Sections were incubated (overnight, 4°C) in anti-dicer or anti-eIF2c antibodies (1:100) in blocking buffer with gentle agitation, washed 5 × 5 min with working buffer (blocking buffer diluted 1:10), incubated in donkey anti-rabbit secondary antibody conjugated to fluorescein (1:100, 1 h, Jackson ImmunoResearch, West Grove PA, USA), rinsed, mounted on glass slides and coverslipped using gelvatol. Sections were viewed on a laser scanning confocal microscope (Bio-Rad 1024 MRC or Radiance 2000) using 63 × oil objective, n.a. = 1.4. As a negative control, the primary antibody was omitted or pre-immune serum was used.

Electron microscopic immunocytochemistry

Animals were perfused and postfixed as above with 4% paraformaldehyde in phosphate-buffered saline containing 0.1% glutaraldehyde. Sagittal vibratome sections were cut at 100 μm. Anti-dicer or anti-eIF2c antibody incubation was performed as above except that the blocking buffer was phosphate-buffered saline containing 1% bovine serum albumin, 3% normal goat serum, 0.1% Triton and 1% cold water fish gelatin (Sigma). Sections were washed 5 × 5 min in working buffer at 4°C, then incubated in biotinylated goat anti-rabbit IgG (1:100, 3 h, 4°C, Vector Laboratories, Burlingame, CA, USA) in working buffer, washed, then incubated in streptavidin–biotin complex (ABC kit; Vector Laboratories, 1 h, room temperature). Sections were rinsed 2 × 5 min in phosphate-buffered saline, 3 × 10 min in 0.1 M Tris-HCl buffer (pH 7.4), followed by 10–20-min incubation in diaminobenzidine (0.5 mg/mL) to which 0.0005% hydrogen peroxide was just added. As a negative control, the primary antibody was omitted. Tissue was embedded in Durcupan ACM resin (EM Sciences, Hatfield, PA, USA) as described (Martone *et al*. 1997). Ultrathin sections were cut at 80–100 nm on a Leica ultramicrotome (Leica Ultracut UCT) and examined without further heavy metal staining on a JEOL 1200fx transmission electron microscope at an accelerating voltage of 100 KeV.

Hippocampal slices

Slices from adult mice (400-μm thick) were incubated in calcium-free artificial CSF for 15 min, 35°C, incubated in artificial CSF containing 2 mM calcium for 1 h, 35°C in the presence or absence of calpeptin, then exposed to NMDA (50 μM) for 10–30 min (Seubert *et al*. 1988; Hoffman *et al*. 1998) in the continued presence or absence of calpeptin.

Results

Dicer and eIF2c are expressed in the somatodendritic component of large neurons

A polyclonal antibody was raised against the C-terminal peptide sequence of dicer, affinity purified, and characterized. In western blots of brain cytosol, anti-dicer recognized several bands including two major bands (Fig. 1a) – a band at 220 kDa which co-migrated with recombinant dicer (recombinant dicer appears slightly larger on gels, probably because it contains a His tag), and a smaller band at 125 kDa.

Because more than one dicer-immunoreactive band was detected in brain extracts, we raised another anti-dicer antibody in chickens (Aves Laboratories, Inc., Tigard,

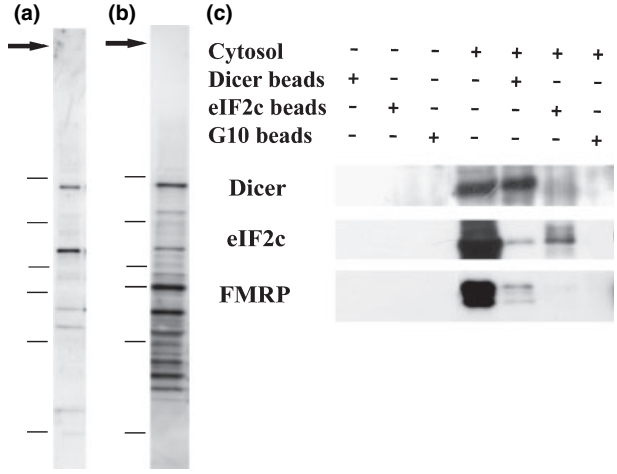

Fig. 1 Immunoblotting of dicer in adult mouse brain. (a) Cytosol fraction (20 000 *g*) prepared under reducing conditions (1% dithiothreitol) and immunoblotted with rabbit C-terminal anti-dicer antibody (1:1000) followed by goat anti-rabbit IgG-peroxidase (1:30 000) and visualized with ECL-Plus.)b) Cytosol immunoblotted with chicken anti-dicer antibody (1:30 000) followed by goat anti-chicken IgG-peroxidase (1:30 000). Arrows on the left indicate the position of the top of the gel. Marks indicate moleclar weight standards at 250, 150, 100, 75, 50, 37 kDa. In both cases, no bands were seen when primary antibody was omitted. (c) Cytosol (concentrated by ammonium sulfate precipitation) was immunoprecipitated using C-terminal anti-dicer, anti-eIF2c or anti-reelin (G10) antibodies coupled covalently to agarose beads (see Materials and methods). Equal fractions of the samples were loaded in 4–15% Tris-HCl acrylamide gel, and immunoblotted with rabbit anti-dicer antibody (as above), or rabbit anti-eIF2c antibody (1:50 000) followed by goat anti-rabbit IgG-peroxidase (1:50 000), or mouse anti-FMRP antibody (1:3000) followed by goat anti-mouse IgG-peroxidase (1:5000). FMRP, fragile X mental retardation protein.

Oregon, USA) that reacts with a peptide (1389–1404) located between the first and second RNAse III domains. This anti-dicer antibody confirmed that the 220 and 125 kDa bands represent forms of dicer, as it recognized these bands in western blotting of brain cytosol (Fig. 1b) and in material immunopreciptated by the C-terminal antibody. Full-length dicer was also recognized by two commercial anti-dicer antibodies that react with more N-terminal epitopes (Imgenex, antibody raised against a mixture of peptides at 132–150 and 1017–1033; and Center for Biomedical Inventions, University of Texas-Southwestern, antibody raised against a fusion protein at 730–829). All four anti-dicer antibodies recognized several smaller bands, suggesting that dicer undergoes some fragmentation under physiologic conditions (Figs 1a and b and data not shown). As presented below, immunoprecipitated brain dicer expressed RNAse III activity and generated 22 nt products. Brain dicer also bound specifically to poly IC agarose beads (Wagner *et al*. 1971), a synthetic double-stranded RNA that binds dicer but is not a substrate (Provost *et al*. 2002), but not to poly C beads (Sigma) (data not shown). Thus, we conclude that the C-terminal anti-dicer antibody does recognize authentic dicer specifically in adult mouse brain. As a final control for antibody specificity, we down-regulated dicer in HEK 293T cells using siRNAs, and found that the dicer-immunoreactive 220 kDa protein band as well as several of the smaller dicer-immunoreactive fragments detected with both anti-dicer antibodies were specifically decreased in abundance (Fig. S1).

In co-immunoprecipitation experiments using brain cytosol, C-terminal anti-dicer antibody specifically brought down detectable amounts of eIF2c and FMRP protein (Fig. 1c), suggesting that a portion of dicer, eIF2c and FMRP in brain are bound to each other, presumably as part of the RISC complex (Doi *et al*. 2003). Similarly, anti-eIF2c antibody brought down dicer and FMRP (Fig. 1c) – although FMRP was barely detectable in eIF2c immunoprecipitates, it is possible that the anti-eIF2c antibody binds close to the FMRP-binding site, or that the buffer employed (containing excess EDTA) disrupts FMRP–eIF2c association more than FMRP–dicer association.

Immunocytochemistry using the C-terminal anti-dicer antibody with fluorescence detection and confocal microscopy revealed that dicer is expressed in many brain regions, in a punctate pattern in the somatodendritic compartment of large neurons, some interneurons and endothelial cells (Figs 2a, c and e). Neuropil was prominently labeled but only light staining was evident in astrocytes, oligodendrocytes and white matter (Fig. S2). Anti-eIF2c antibody showed prominent Golgi and ER expression, which is consistent with its reported distribution in other cell types (Cialuk *et al*. 1999), and was detectable throughout the somatodendritic regions of large projection neurons (Figs 2b, d and f). Electron microscopy immunocytochemistry using peroxidase-based detection confirmed that dicer-like immunoreactivity was present

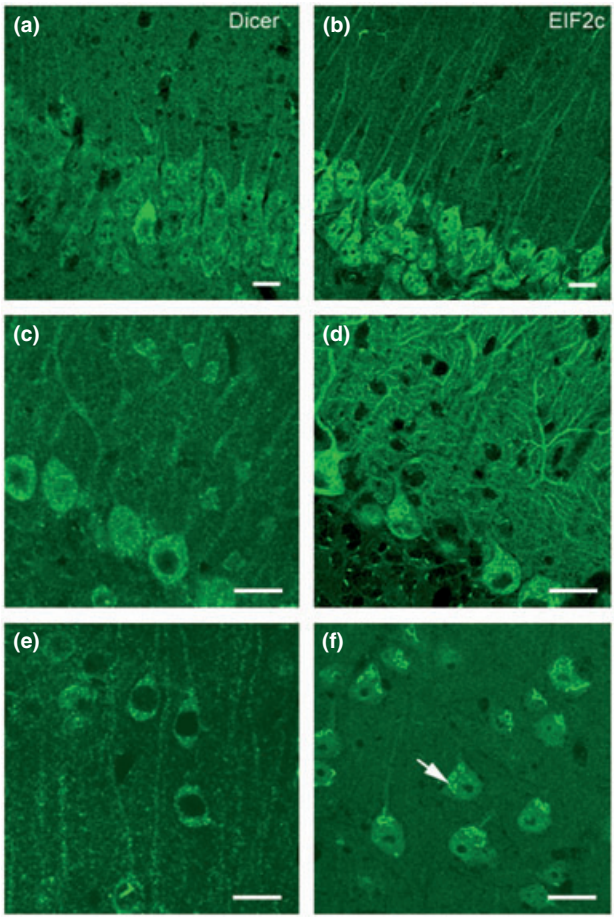

Fig. 2 Immunolabeling for dicer and eIF2c in adult mouse brain. (a, c, e) Anti-dicer antibody, (b, d, f) anti-eIF2c antibody labeling. (a, b) hippocampal area CA1, (c, d) cerebellar cortex and (e, f) neocortex. Although labeling for the two proteins was generally found in the same cells and subcellular locations, labeling for eIF2c was much stronger than for dicer, particularly in cerebellar (d) cortex, where Purkinje cells were intensely labeled throughout the dendritic tree and dendritic spines. Labeling for dicer was more uniform in the various cell layers of the cerebellar cortex (c). eIF2c exhibited a prominent subcellular localization that likely corresponded to the Golgi apparatus (arrow in f). In contrast, dicer showed a punctate distribution more uniformly in the cytoplasm. Scale bars = 20 μm.

within dendritic spines and appeared to be particularly associated with PSDs (Figs 3a and c). eIF2c was also prominent in spines (Fig. 3b).

Although the nucleus was generally devoid of dicer immunoreactivity in most brain regions, granule neurons of the dentate gyrus consistently showed intranuclear dicer and eIF2c immunoreactivity in both diffuse and organellar patterns (Fig. S2). As well, in certain neuronal cell types, notably cortical pyramidal neurons, intense streaks of dicer immunoreactivity were commonly found within a subset of nuclei (Fig. 2e); these streaks were *not* stained for eIF2c (not shown). Further investigation of these phenomena is

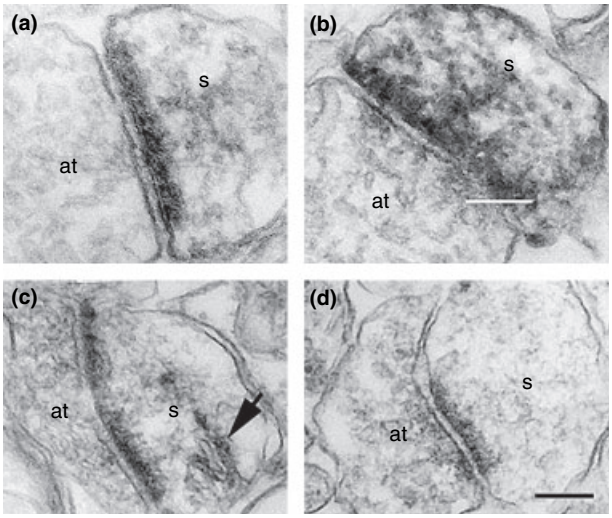

Fig. 3 Electron microscopy localization of dicer and eIF2c in dendritic spines in cortex and hippocampal area CA1. The distribution of dicer (a, c) tended to be more discrete than eIF2c (b). In the cortical spine in (c), a deposit of label can be seen surrounding the spine apparatus (arrow). Post-synaptic densities were heavily labeled for both proteins, much greater than the slight contrast due to heavy metal staining that can be seen in tissue labeled without the primary antibody (d). s, spine head; at, axon terminal. Scale bar = 200 nm.

warranted in view of the evidence that dicer isoforms have nuclear functions in lower organisms (e.g. Reinhart and Bartel 2002), and that dicer can enter the nucleus in mammals as well (Meister *et al*. 2004).

Dicer has RNAse III activity that is enhanced by calpain

Recombinant dicer and immunoprecipitated brain dicer both exhibited typical dicer-like RNAse III activity that was Mg-dependent and resulted in formation of 22 nt products (Fig. 4 and Fig. S3). In contrast, when RNAse III assays were conducted using crude cytosol, no accumulation of small RNA products occurred, even when recombinant dicer was added (Fig. S3). This indicates that component(s) present in the cytosol are able to degrade the small RNAs formed from dicer.

Provost *et al*. (2002) and Zhang *et al*. (2002) demonstrated that brief proteinase K treatment of recombinant dicer increases its RNAse III activity. Because calpain participates in neuronal responses to synaptic activation (Lynch and Baudry 1987; Chan and Mattson 1999), we asked if calpain may also cleave dicer and activate dicer RNAse III activity. Calpain I treatment of recombinant dicer caused the transient appearance of fragments at 75 and 50 kDa and the stable accumulation of a single 28 kDa fragment that includes the C-terminus (Fig. 5a). On the basis of its size, the end-digest fragment is predicted to comprise the second RNAse III catalytic domain and the dsRNA binding domain. Calpain I treatment of recombinant dicer markedly increased RNAse III activity which lasted at least 24 h (Figs 4a and b).

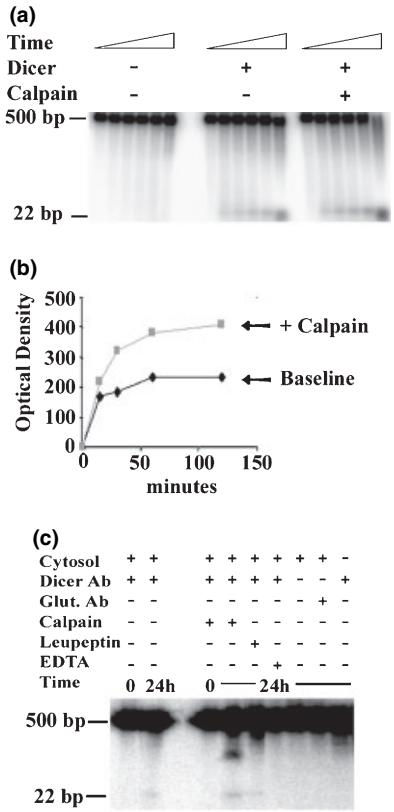

Fig. 4 Calpain I stimulates dicer RNAse III activity. (a) Recombinant dicer was assayed for RNAse III activity as described in Methods. Reactions were stopped after 0, 15, 30, 60, 120 min, and 24 h by adding gel loading buffer, separated on a 4–20% Criterion-TBE gel, and autoradiographed. Panel at left: when dicer was omitted, no activity was detected. Middle panel: baseline dicer assay shows progressive formation of 22 nt products over time. Panel at right: calpain I (3 U/mL) treatment caused a greater loss of 500 bp substrate, and more formation of 22 nt product, relative to the baseline assay. Calpain alone had no RNAse III activity (not shown). (b) Optical density measurements of the 22 nt product (from the autoradiograms in a) are plotted for the first 2 h of incubation. (c) Brain dicer was immunoprecipitated from cytosol using anti-dicer antibody (see Methods) and assayed for RNAse III activity. As negative controls, no activity was detected when anti-dicer antibody was omitted, or when rabbit anti-glutamate antibody (Sigma) was used instead for immunoprecipitation. Also, no RNAse III activity was observed in the absence of Mg, or in the presence of excess EDTA (see Fig. S3). Calpain treatment increased the amount of 22 nt product observed; this increase was blocked in the presence of the calpain inhibitor leupeptin.

When brain dicer was purified from adult mouse brain cytosol by immunoprecipitation with C-terminal anti-dicer antibody, and then treated with calpain, RNAse III activity was stimulated as well (Fig. 4c). Calpain treatment decreased the dicer-immunoreactive bands, and caused the appearance of a 75 kDa dicer-immunoreactive fragment (Fig. 5b). However, no 28 kDa fragment was detected, suggesting that some of the potential proteolytic sites in brain dicer are

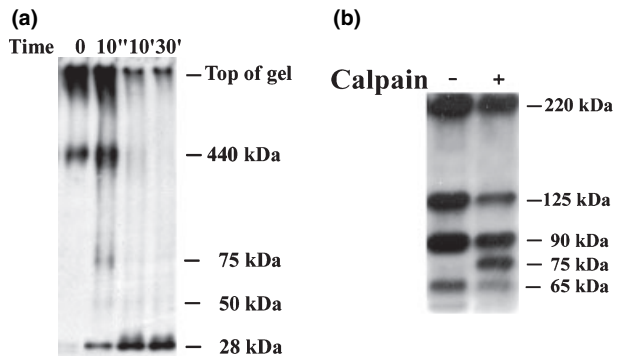

Fig. 5 Calpain I cleaves dicer. (a) Recombinant dicer (0.5 U) was incubated with calpain I (3 U/mL) in the presence of 2.5 mM $CaCl_2$ in 10 μL at 37°C, for 10 s, 10 min, or 30 min. Reactions were stopped by adding an equal volume of sodium dodecyl sulfate–polyacrylamide gel electrophoresis loading buffer, electrophoresed in a 4–20% gradient polyacrylamide-Tris gel under non-reducing conditions, and immunoblotted using anti-dicer antibody. (b) Dicer was immunoprecipitated from ammonium sulfate concentrated cytosol, and incubated with vs. without calpain I (3 U/mL) in the presence of 2.5 mM $CaCl_2$ in at 37°C, for 30 min. Reactions were stopped by adding an equal volume of sodium dodecyl sulfate–polyacrylamide gel electrophoresis loading buffer, electrophoresed in a 4–20% gradient polyacrylamide-Tris gel under reducing conditions, and immunoblotted using C-terminal anti-dicer antibody.

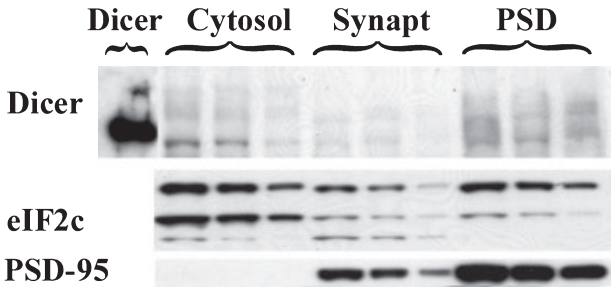

Fig. 6 Expression of dicer and eIF2c in brain subcellular fractions. Recombinant dicer, brain cytosol (20 000 *g* supernatant is shown here, but 200 000 *g* supernatant is similar), synaptosomes, and postsynaptic densities (PSD) were separated by sodium dodecyl sulfate–polyacrylamide gel electrophoresis under reducing conditions and immunoblotted with anti-dicer antibody (top), anti-eIF2c (middle) or anti-PSD-95 (bottom). Each sample was loaded on three lanes with decreasing amounts of protein (40, 20, 10 μg) to ensure that band intensities were not saturated. Top blot: monomer and larger forms of brain dicer are particularly enriched in PSDs. Middle blot: eIF2c-immunoreactive bands are seen at 140 and 94 kDa with traces at 70 kDa. eIF2c-like bands are richest in cytosol and are detected (though not enriched) in PSDs. Bottom blot: positive control: PSD-95 protein is undetectable in cytosol and highly enriched in the PSD fraction.

protected, e.g. by dicer-associated proteins brought down together by the antibody.

In both recombinant and immunopurified brain dicer, the production of small RNA products in the RNAse III assay was non-linear over time (Fig. 4), which is consistent with end-product inhibition (Provost *et al*. 2002; Zhang *et al*. 2002). Calpain treatment did not alter the shape of this non-linear curve (Fig. 4b).

Dicer is enriched but enzymatically inactive in postsynaptic densities, and is released in active form by calpain

Subcellular fractionation of adult mouse brain gave evidence that was consistent with immunocytochemistry, and showed that dicer was particularly enriched in purified postsynaptic densities (PSDs) (Fig. 6, top). A dicer-immunoreactive band was also enriched in PSDs that was approximately twice the size of native dicer, but which was not affected by boiling and reduction of the sample (Fig. 6); it is not clear whether this represents dimeric dicer or a sodium dodecyl sulfate-resistant complex of dicer with another protein(s). An antibody against the RISC component eIF2c showed bands at 140 kDa and 94 kDa with faint staining at 70 kDa. eIF2c-like bands are richest in cytosol but are also readily detected in PSDs (Fig. 6, middle). The eIF2c bands have not been characterized further in the present study, but the primary translation product observed in reticulocyte lysates migrates at 140 kDa (Zou *et al*. 1998) whereas eIF2c1 and eIF2c2 run predominantly as 94 kDa species in western blots of tissue extracts and have been identified as RISC components (Cialuk *et al*. 1999; Doi *et al*. 2003; Nelson *et al*. 2004).

Intriguingly, no detectable RNAse III activity was detected in purified PSDs (Fig. 7b). However, after treating purified PSDs with calpain I for 10 min, the preparation was subsequently quite active in cutting the dsRNA template (Fig. 7b). This indicates that much of the dicer protein associated with the PSD is cryptic (not active or not accessible to dsRNA) until acted upon by calpain. When purified PSDs were incubated directly with calpain I, dicer disappeared from the PSDs, whereas dicer-immunoreactive bands at 220 kDa and fragments at 150, 140, 75 and 50 kDa were liberated into the supernatant (Fig. 7a, top). Treating purified PSDs with calpain I caused the disappearance of the eIF2c 140 kDa band, concomitant with the appearance of eIF2c 94 kDa in the supernatant (Fig. 7a, bottom).

Neuronal stimulation causes the formation of a 75 kDa dicer-immunoreactive fragment in a calcium- and calpain-dependent manner

Incubating synaptoneurosomes in the presence of 2.5 mM calcium caused a rapid decrease in dicer 220 and 125 kDa and a corresponding appearance of a new dicer fragment at 75 kDa (Fig. 8; this corresponds to the dicer fragment formed by calpain treatment of immunopurified brain dicer, Fig. 5b). These changes were blocked by adding the thiol protease inhibitor leupeptin or the cell-permeable calpain

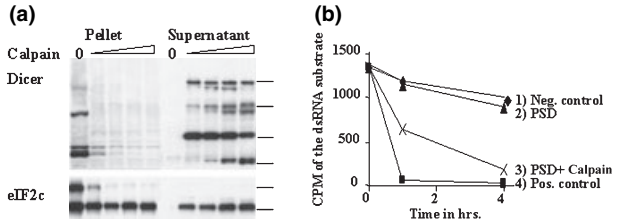

Fig. 7 Calpain I liberates dicer and eIF2c from postsynaptic densities (PSDs) and uncovers cryptic RNAse III activity. (A) Purified PSDs were treated with increasing concentrations of calpain I (0, 0.6, 3, 6, 12 units/mL) for 30 min at 37°C, and spun down at 20 000 *g*, 30 min, 4°C. Pellet and supernatant were each precipitated in methanol, dissolved in sodium dodecyl sulfate–polyacrylamide gel electrophoresis buffer plus 1% dithiothreitol, loaded on 4–20% gradient polyacrylamide gels (equal fractions per lane) and immunoblotted with anti-dicer antibody (top) or anti-eIF2c (bottom). Top: calpain digestion caused the loss of nearly all of the dicer associated with the PSD and liberated a number of dicer-immunoreactive bands into the supernatant, including a band that co-migrated with full-length dicer (220 kDa) and smaller discrete bands at 150, 140, 75, and 50 kDa. Marks indicate the position of molecular mass standards at 250, 150, 75, and 50 kDa. Bottom: the eIF2c 140 kDa band associated with the PSD is cleaved by calpain, occurring in parallel with the release of a eIF2c 94 kDa band into the supernatant. Marks indicate 140 and 94 kDa. (b) Purified PSDs were treated with or without calpain I (3 U/mL) for 30 min, 37°C, then leupeptin (10 μg/mL) was added to stop residual calpain activity before conducting a RNAse III assay (see Methods). As a negative control, a tube was run with no PSDs added, and as a positive control, an extra tube was assayed using recombinant dicer. Reactions were stopped at 1 and 4 h by extracting RNA with Trizol (Invitrogen) and resuspended in equal volumes of loading buffer. Samples were separated on 4–20% Criterion-TBE gels, and the 500 bp dsRNA substrate bands were counted in a scintillation counter. Whereas purified PSDs were no different than the negative control group, the calpain-treated PSDs showed significant RNase III activity.

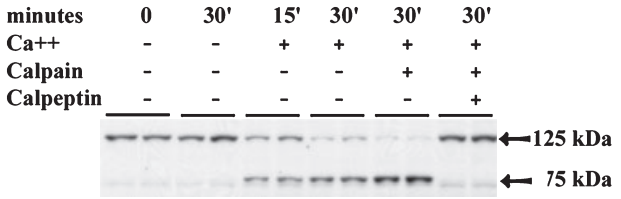

Fig. 8 Calpain-dependent cleavage of dicer in synaptoneurosomes. Synaptoneurosomes were incubated in HB buffer (lacking EDTA and protease inhibitors) at 37°C in the presence of $CaCl_2$ 2.5 mM, calpain I (3 U/mL), or the specific calpain inhibitor calpeptin (100 μg/mL). Reactions were stopped at 15 or 30 min by methanol precipitation; samples were resuspended in sodium dodecyl sulfate–polyacrylamide gel electrophoresis buffer under reducing conditions and immunoblotted with anti-dicer antibody. Experiments were run in duplicate (each lane is a separate sample). Calcium treatment caused a rapid decrease in a 125 kDa fragment with the appearance of a new fragment at 75 kDa. Decreases were also observed in dicer 220 and 50 kDa (not shown).

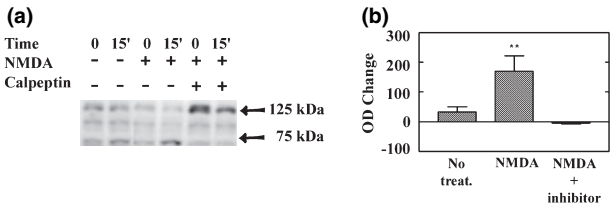

Fig. 9 Calpain-dependent cleavage of dicer in NMDA stimulated hippocampal slices. (a) Hippocampal slices (six slices pooled per sample) were pre-incubated with or without calpeptin (100 μg/mL) for 1 h and treated with or without NMDA (50 μM) for 15 min (see Methods). Pooled slices taken either before (time 0) or after treatment were homogenized in HB, spun (20 000 *g*, 20 min, 4°C), and supernatant was precipitated in methanol, dissolved in sodium dodecyl sulfate–polyacrylamide gel electrophoresis buffer plus dithiothreitol and loaded for immunoblotting using anti-dicer antibody. (b) Changes in the 75 kDa band after no treatment, NMDA treatment, or NMDA plus calpeptin. In each experiment, the optical density (OD) of the 75 kDa bands was normalized to the value of the 'No treatment at $t = 0$' lane. Histogram shows the mean change in OD (± SEM) from $t = 0$ to $t = 15$ min for each condition in five independent experiments. **ANOVA indicated a significant effect of treatment ($F_{2,8} = 10.29$, $p < 0.01$); Newman–Keuls tests showed that the NMDA group was significantly higher than both the No Treatment and NMDA + inhibitor groups ($p < 0.01$), which did not differ from each other.

selective inhibitor calpeptin. Also, adding exogenous calpain I to synaptoneurosomes in the presence of calcium enhanced the formation of the 75 kDa fragment beyond what was produced by endogenous calpain alone (Fig. 8).

In a second paradigm, acute hippocampal slices were exposed to NMDA for 15 min. Slight but detectable formation of the 75 kDa band occurred during incubation even in the baseline condition – this probably reflects cellular damage from the slicing procedure, since it could be prevented by pre-incubating slices in calpeptin (Fig. 9). Despite this baseline, NMDA exposure clearly elicited a large increase in the 75 kDa dicer fragment in a manner that was blocked by calpeptin (Fig. 9).

Discussion

The present study reports that in adult mouse brain, dicer, the rate-limiting enzyme in formation of small RNAs, is expressed in the somatodendritic domain of projection neurons, including the dendritic spines, and is enriched at postsynaptic densities (PSDs). Dicer in purified PSDs is cryptic but calpain treatment causes the liberation of enzymatically active dicer and dicer-immunoreactive fragments, as well as the RISC component eIF2c. NMDA stimulation of acute hippocampal slices, and calcium stimulation of synaptoneurosomes, causes the appearance of a 75 kDa dicer fragment that is calcium-dependent and prevented by the calpain inhibitor calpeptin. These findings immediately suggest the following testable model: (i)

glutamate or other neurotransmitter activity at synapses causes a local increase of intracellular calcium levels within the postsynaptic neuron; (ii) this calcium increase needs to be sufficient to activate calpain; (iii) calpain liberates active dicer and eIF2c from the PSD.

There are a number of ways in which calpain may affect dicer function. First, mobilizing dicer and eIF2c may set them free to act on microRNA precursors or sense–antisense RNA pairs to form small RNAs that, in turn, may regulate translation or stability of nearby mRNAs at dendritic spines. MicroRNAs have been found to be associated with FMRP, dicer, BC1 and polysomes in neurons (Doi *et al*. 2003; Jin *et al*. 2004; Kim *et al*. 2004; Nelson *et al*. 2004), all of which are located near dendritic spines. Indeed, we showed the presence of eIF2c throughout spines, and polysomes have been observed to be present within the heads of dendritic spines following tetanic stimulation (Ostroff *et al*. 2002), so that small RNA pathways could act quite locally near the PSD. The NMDA–calcium–calpain system is regarded as a high threshold trigger to initiate changes that result in stable long-term potentiation (LTP) (Lynch and Baudry 1987). Therefore, it is appealing to hypothesize that acute effects of calpain on dicer should act as a highly localized, phasic, high-threshold trigger that leads to formation of small RNAs near synapses – and that once formed, the small RNAs should be relatively long-lasting and subsequently independent of ongoing dicer activity. In order to test this idea, however, more needs to be known in neurons regarding the synthesis, transport, localization and turnover of small RNAs (microRNAs and siRNAs) and their precursors. It is intriguing that steady-state tissue levels of microRNA precursors are very low relative to mature microRNAs (e.g. Schmittgen *et al*. 2004), so overall microRNA levels may be determined primarily by microRNA turnover rates. Synthetic siRNAs transfected into postmitotic neurons appear to be stable for at least 3 weeks (Omi *et al*. 2004) – an effect that is presumably independent of dicer activity – so one would expect microRNAs to be similarly stable, once formed and incorporated into RISC.

Second, calpain may enhance the intrinsic RNAse III activity of dicer via generating highly active fragments. Calpain certainly increases the enzymatic activity of purified recombinant and brain dicer *in vitro*; however, we have not yet been able to demonstrate a robust increase in RNAse III activity in crude cytosol (unpublished observations). Third, insofar as a portion of dicer is a part of the RISC complex, calpain acting on dicer may have an effect on RISC function. Fourth, dicer and a number of small RNA pathway components may modulate or execute functions of FMRP (e.g. Jin *et al*. 2004; Xu *et al*. 2004).

Fifth, dicer contains strongly predicted nuclear localization signals (Nicholson and Nicholson 2002). Whereas the intact protein was initially reported to be exclusively cytoplasmic, dicer has recently been reported to enter the nucleus in certain cell types (Meister *et al*. 2004), and we now show that dicer immunoreactivity is observed in the nucleus of certain neuronal cell types (see Results). Finally, dicer is known to bind directly to 5-lipoxygenase (Provost *et al*. 1999), which is also responsive to changes in neuronal activity (Manev *et al*. 2000), and may have functions apart from small RNA pathways.

In conclusion, the present study sets the stage for a detailed examination of the role of small RNA pathways in synaptic functions, particularly in plasticity and learning. We hope to learn whether mice undergoing acute synaptic stimulation (e.g. following intense sensory stimulation or during olfactory discrimination learning) will exhibit formation of the dicer 75 kDa fragment, enhance cleavage of microRNA precursors locally at specific dendritic spines, and cause an increase in small RNAs associated with activated synapses. Also, we hope to learn if interfering with dicer activity in adult mice will inhibit aspects of synaptic plasticity and learning *in vivo*. Insofar as calpain activation also accompanies adverse events in brain such as ischemia and excitotoxity, changes in dicer may be expected to occur during certain pathologic situations.

The present study is the first report of a physiological mechanism to dynamically regulate dicer activity in any living cell. Given its widespread roles in cellular biology, it will be interesting to learn whether the calcium-calpain system may regulate dicer activity not only in neurons but in other cell types as well.

Supplementary Material

The following material is available from http://www.blackwell-science.com/products/journals/suppmat/JNC/JNC3224/JNC3224sm.htm

Figure S1. Down-regulation of dicer using siRNAs in HEK 293T cells causes a loss of dicer-immunoreactivity as detected with anti-dicer C-terminal antibody.

Figure S2. Immunolocalization of dicer (green) in multiple brain regions. (a) caudoputamen; (b) hippocampal area CA1; (c) neocortex; (d) dentate gyrus; (e) higher magnification view of neocortex; (f) higher magnification view of dentate gyrus granule cells. f, fiber fascicle; pcl, pyramidal cell layer; gcl, granule cell layer; ml, molecular layer. Scale bars in a–d = 100 μm; scale bars in e and f = 20 μm.

Figure S3. RNAse III activity assay in lysed synaptoneurosomes.

Acknowledgements

Supported by NIH grants DA15450, LM07292 and DC005793. This Human Brain Project/Neuroinformatics research is funded jointly by the National Library of Medicine and the National Institute of Mental Health. Some of the work was conducted at the National Center for Microscopy and Imaging Research supported by the

National Institutes of Health (NCRR P41 RR04050). Thanks to Ruth Jessen for assistance with slice experiments, and Christina Floreani for assistance with subcellular fractionation.

References

Bartel D. P. (2004) MicroRNAs: genomics, biogenesis, mechanism, and function. *Cell* **116**, 281–297.

Bernstein E., Caudy A. A., Hammond S. M. and Hannon G. J. (2001) Role for a bidentate ribonuclease in the initiation step of RNA interference. *Nature* **409**, 363–366.

Caudy A. A., Myers M., Hannon G. J. and Hammond S. M. (2002) Fragile X-related protein and VIG associate with the RNA interference machinery. *Genes Dev.* **16**, 2491–2496.

Caudy A. A., Ketting R. F., Hammond S. M., Denli A. M., Bathoorn A. M., Tops B. B., Silva J. M., Myers M. M., Hannon G. J. and Plasterk R. H. (2003) A micrococcal nuclease homologue in RNAi effector complexes. *Nature* **425**, 411–414.

Chan S. L. and Mattson M. P. (1999) Caspase and calpain substrates: roles in synaptic plasticity and cell death. *J. Neurosci. Res.* **58**, 167–190.

Cialuk D. E., Tahbaz N., Hendricks L. C., DiMattia G. E., Hansen D., Pilgrim D. and Hobman T. C. (1999) GERp95, a membrane-associated protein that belongs to a family of proteins involved in stem cell differentiation. *Mol. Biol. Cell* **10**, 3357–3372.

Doi N., Zenno S., Ueda R., Ohki-Hamazaki H., Ui-Tei K. and Saigo K. (2003) Short-interfering-RNA-mediated gene silencing in mammalian cells requires Dicer and eIF2C translation initiation factors. *Curr. Biol.* **13**, 41–46.

Dostie J., Mourelatos Z., Yang M., Sharma A. and Dreyfuss G. (2003) Numerous microRNPs in neuronal cells containing novel microRNAs. *RNA* **9**, 180–186.

Dykxhoorn D. M., Novina C. D. and Sharp P. A. (2003) Killing the messenger: short RNAs that silence gene expression. *Nat. Rev. Mol. Cell. Biol.* **4**, 457–467.

Greenough W. T., Klintsova A. Y., Irwin S. A., Galvez R., Bates K. E. and Weiler I. J. (2001) Synaptic regulation of protein synthesis and the fragile X protein. *Proc. Natl Acad. Sci. USA* **2001**, 7101–7106.

Hoffman K. B., Larson J., Bahr B. A. and Lynch G. (1998) Activation of NMDA receptors stimulates extracellular proteolysis of cell adhesion molecules in hippocampus. *Brain Res.* **811**, 152–155.

Hommel J. D., Sears R. M., Georgescu D., Simmons D. L. and DiLeone R. J. (2003) Local gene knockdown in the brain using viral-mediated RNA interference. *Nat. Med.* **9**, 1539–1544.

Ishizuka A., Siomi M. C. and Siomi H. (2002) A Drosophila fragile X protein interacts with components of RNAi and ribosomal proteins. *Genes Dev.* **16**, 2497–2508.

Jin P., Zarnescu D. C., Ceman S., Nakamoto M., Mowrey J., Jongens T. A., Nelson D. L., Moses K. and Warren S. T. (2004) Biochemical and genetic interaction between the fragile X mental retardation protein and the microRNA pathway. *Nat. Neurosci.* **7**, 113–117.

Kim J., Krichevsky A., Grad Y., Hayes G. D., Kosik K. S., Church G. M. and Ruvkun G. (2004) Identification of many microRNAs that copurify with polyribosomes in mammalian neurons. *Proc. Natl Acad. Sci. USA* **101**, 360–365.

Krichevsky A. M. and Kosik K. S. (2002) RNAi functions in cultured mammalian neurons. *Proc. Natl Acad. Sci. USA* **99**, 11 926–11 929.

Krichevsky A. M., King K. S., Donahue C. P., Khrapko K. and Kosik K. S. (2003) A microRNA array reveals extensive regulation of microRNAs during brain development. *RNA* **9**, 1274–1281.

Lagos-Quintana M., Rauhut R., Yalcin A., Meyer J., Lendeckel W. and Tuschl T. (2002) Identification of tissue-specific microRNAs from mouse. *Curr. Biol.* **12**, 735–739.

Lai E. C. (2003) microRNAs: runts of the genome assert themselves. *Curr. Biol.* **13**, R925–R936.

Lynch G. and Baudry M. (1987) Brain spectrin, calpain and long-term changes in synaptic efficacy. *Brain Res. Bull.* **18**, 809–815.

Makimura H., Mizuno T. M., Mastaitis J. W., Agami R. and Mobbs C. V. (2002) Reducing hypothalamic AGRP by RNA interference increases metabolic rate and decreases body weight without influencing food intake. *BMC Neurosci.* **3**, 18.

Manev H., Uz T. and Qu T. (2000) Early Upregulation of Hippocampal 5-lipoxygenase Following Systemic Administration of Kainate to Rats. *Exp. Gerontol.* **35**, 1201–1209.

Martone M. E., Pollock J. A., Jones Y. Z. and Ellisman M. H. (1996) Ultrastructural localization of dendritic messenger RNA in adult rat hippocampus. *J. Neurosci.* **16**, 7437–7446.

Martone M. E., Holash J. A., Bayardo A., Pasquale E. B. and Ellisman M. H. (1997) Immunolocalization of the receptor tyrosine kinase EphA4 in the adult rat central nervous system. *Brain Res.* **771**, 238–250.

Meister G., Landthaler M., Patkaniowska A., Dorsett Y., Teng G. and Tuschl T. (2004) Human Argonaute2 mediates RNA cleavage targeted by miRNAs and siRNAs. *Mol. Cell* **15**, 185–197.

Miska E. A., Alvarez-Saavedra E., Townsend M., Yoshii A., Sestan N., Rakic P., Constantine-Paton M. and Horvitz H. R. (2004) Microarray analysis of microRNA expression in the developing mammalian brain. *Genome Biol.* **5**, R68.

Nelson P. T., Hatzigeorgiou A. G. and Mourelatos Z. (2004) miRNP: mRNA association in polyribosomes in a human neuronal cell line. *RNA* **10**, 387–394.

Nicholson R. H. and Nicholson A. W. (2002) Molecular characterization of a mouse cDNA encoding Dicer, a ribonuclease III ortholog involved in RNA interference. *Mamm. Genome* **13**, 67–73.

Omi K., Tokunaga K. and Hohjoh H. (2004) Long-lasting RNAi activity in mammalian neurons. *FEBS Lett.* **558**, 89–95.

Ostroff L. E., Fiala J. C., Allwardt B. and Harris K. M. (2002) Polyribosomes redistribute from dendritic shafts into spines with enlarged synapses during LTP in developing rat hippocampal slices. *Neuron* **35**, 535–545.

Provost P., Samuelsson B. and Radmark O. (1999) Interaction of 5-lipoxygenase with cellular proteins. *Proc. Natl Acad. Sci. USA* **96**, 1881–1885.

Provost P., Dishart D., Doucet J., Frendewey D., Samuelsson B. and Radmark O. (2002) Ribonuclease activity and RNA binding of recombinant human Dicer. *EMBO J.* **21**, 5864–5874.

Reinhart B. J. and Bartel D. P. (2002) Small RNAs correspond to centromere heterochromatic repeats. *Science* **297**, 1831.

Schmittgen T. D., Jiang J., Liu Q. and Yang L. (2004) A high-throughput method to monitor the expression of microRNA precursors. *Nucleic Acids Res.* **32**, e43.

Sempere L. F., Freemantle S., Pitha-Rowe I., Moss E., Dmitrovsky E. and Ambros V. (2004) Expression profiling of mammalian microRNAs uncovers a subset of brain-expressed microRNAs with possible roles in murine and human neuronal differentiation. *Genome Biol.* **5**, R13.

Seubert P., Larson J., Oliver M., Jung M. W., Baudry M. and Lynch G. (1988) Stimulation of NMDA receptors induces proteolysis of spectrin in hippocampus. *Brain Res.* **460**, 189–194.

Smalheiser N. R. and Collins B. J. (2000) Coordinate enrichment of cranin (dystroglycan) subunits in synaptic membranes of sheep brain. *Brain Res.* **887**, 469–471.

Smalheiser N. R., Manev H. and Costa E. (2001) RNAi and brain function: was McConnell on the right track? *Trends Neurosci.* **24**, 216–218.

Steward O. and Schuman E. M. (2003) Compartmentalized synthesis and degradation of proteins in neurons. *Neuron* **40**, 347–359.

Wagner A. F., Bugianesi R. L. and Shen T. Y. (1971) Preparation of sepharose-bound poly (rI: rC). *Biochem. Biophys. Res. Commun.* **45**, 184–189.

Weiler I. J., Irwin S. A., Klintsova A. Y., Spencer C. M., Brazelton A. D., Miyashiro K., Comery T. A., Patel B., Eberwine J. and Greenough W. T. (1997) Fragile X mental retardation protein is translated near synapses in response to neurotransmitter activation. *Proc. Natl Acad. Sci. USA* **94**, 5395–5400.

Xu K., Bogert B. A., Li W., Su K., Lee A. and Gao F. B. (2004) The fragile X-related gene affects the crawling behavior of Drosophila larvae by regulating the mRNA level of the DEG/ENaC protein pickpocket1. *Curr. Biol.* **14**, 1025–1034.

Yekta S., Shih I. H. and Bartel D. P. (2004) MicroRNA-directed cleavage of HOXB8 mRNA. *Science* **304**, 594–596.

Zhang H., Kolb F. A., Brondani V., Billy E. and Filipowicz W. (2002) Human Dicer preferentially cleaves dsRNAs at their termini without a requirement for ATP. *EMBO J.* **21**, 5875–5885.

Zou C., Zhang Z., Wu S. and Osterman J. C. (1998) Molecular cloning and characterization of a rabbit eIF2C protein. *Gene* **211**, 187–194.